Supporting Information

Yu et al. 10.1073/pnas.1211757110

SI Text

Plant Defense Transcription Factor *WRKY22* Is Negatively Regulated by siRNA-Directed DNA Methylation. To identify candidate defense genes that are directly regulated by RNA-directed DNA methylation (RdDM) we first isolated genes that are flg22-induced and targeted by siRNAs in their promoter regions (Dataset S3). Using this approach, we identified the transcription factor *WRKY22* (Fig. S14), previously implicated in Flagellin-Sensing 2 (FLS2) signaling and *Flagellin-induced Receptor Kinase 1 (FRK1)* regulation (1). This gene carries DNA methylation in its promoter region that is dependent on DNA methyltransferase- but not on Repressor Of Silencing 1 (ROS1) activities (Fig. S15). Interestingly, WRKY22 transcript levels were not altered in untreated DNA methylation-defective mutants (Fig. S2); however, they were enhanced and/or sustained in flg22-treated mutant seedlings impaired in RdDM activity (Fig. S16). Furthermore, flg22-triggered DNA demethylation at the *WRKY22* promoter was correlated with its transcriptional induction in an apparently *ROS1*-independent manner (Figs. S15, S17, and S18), suggesting the possible implication of other DNA demethylases in this regulatory process. Alternatively, flg22-triggered inactivation of RdDM activity might be sufficient to mediate DNA demethylation at this *locus*.

SI Materials and Methods

Plant Growth Conditions and Treatments. Most of the plants used in this study were grown at 21–23 °C with an 8-h photoperiod. They were first grown on plates containing Murashige and Skoog medium (Duchefa) [composition for a 1-L medium (pH = 5.7): 2.3 g MS, 0.5% sucrose, 0.8% agar, 0.5 g Mes, vitamins (Sigma; M7150)], and then transferred to soil at 10 d-postgermination (dpg). Five- to 6-wk-old leaves from different genotypes were then syringe infiltrated with either water or flg22 synthetic peptide (Genscript), at 1-μM concentration. To investigate the kinetics of *WRKY22* and *RMG1* induction in RdDM mutants, seedlings were grown on plates containing MS medium (Duchefa), 0.5% sucrose and 0.8% agar for 10 d (21–23 °C with a 16-h photoperiod) and then transferred into MS liquid medium (two seedlings per 500 μL of medium in wells of 24-well plates) for 48 h. Seedlings were then treated with either water or flg22 peptide at 200 nM concentration (Figs. S11 and S16). For the zebularine experiment, seedlings were grown on plates containing MS medium (Duchefa), 0.5% sucrose, and 0.8% agar for 14 d (21–23 °C with a 16-h photoperiod) in the absence or presence of zebularine at 40 μM (Sigma; Z4775) and then collected for histochemical GUS staining or RT-qPCR analyses (Fig. S3).

Transgenic Plant Materials and DNA Contructs. A 479-bp region from the *AtGP1 LTR*, highly targeted by RdDM, was amplified using primers described in Dataset S2 and the resulting PCR product introduced into the pENTR/D/TOPO entry vector, sequenced, and then recombined into the GATEWAY Binary destination pBGWFS7 vector. *AtGP1 LTR*:*GUS* transgenic lines were generated by transforming Col-0 plants with the pBGWFS7 vector carrying *AtGP1 LTR*:*GUS* construct and one reference line, referred to as *AtGP1 LTR*:*GUS* #16, was subsequently selected based on its sensitivity to the DNA methyltransferase inhibitor zebularine. To generate ROS1–GUS construct, the negative strand covering 15,320,379–15,323,482 base pairs (bp) of chromosome 2 was amplified from gDNA using primers described in Dataset S2, cloned, and sequenced. The cloned ROS1 DNA was then digested with Sal1 and Xba1 and ligated into the corresponding sites of the binary vector pB101.1. This *ROS1–GUS* reporter gene is comprised of ROS1 5′ sequences from −2131 to −1 (from translation start) and 1–975 bp of ROS1 coding region.

Histochemical GUS Staining. Five- to 6-wk-old leaves of *AtGP1 LTR*:*GUS* #16 were syringe infiltrated with either water or flg22 peptide at 1-μM concentration and collected at 24 h posttreatment. They were placed in microplates containing a GUS staining buffer, vacuum infiltrated three times during 15 min, and then incubated overnight at 37 °C. Leaves were subsequently washed several times in 70% ethanol. Six leaves of each plant were analyzed in three independent experiments. Five- to 6-wk-old ROS1–GUS nontreated leaves were collected, GUS stained, and washed similarly.

Bacterial Infections. Bacterial infections were performed by syringe infiltration or wound inoculation on 5- to 6-wk-old *Arabidopsis* leaves of different genotypes. *Pseudomonas syringae* pv. *tomato* strain DC3000 (*Pto* DC3000) and a GFP-tagged *Pto* DC3000, referred to as *Pto* DC3000–GFP, were used for this study. For syringe-inoculation assay, *Pto* DC3000 was used at a concentration of 10^5 colony-forming units per milliliter (cfu/mL) and bacterial titers were monitored by serial dilution assays. For wound inoculation, *Pto* DC3000–GFP was used at a concentration of 5×10^7 cfu/mL and inoculated in either midveins or secondary veins with a toothpick. Bacterial propagation was then analyzed by monitoring GFP signal under a UV light using an Olympus MV 10× macrozoom and pictures were taken with a CCD camera AxioCam Mrc Zeiss with a GFP filter (exposure time 347 ms). To determine the presence of *Pto* DC3000–GFP in xylem vessels, transversal sections of leaves were conducted by cutting polystyrene rod containing leaf transversally with a razor blade.

Real-Time RT-PCR Analyses. Total RNA was extracted using RNeasy Plant Mini kit (Qiagen). RNA samples were reverse transcribed into cDNA using SuperScript III Reverse Transcriptase (Invitrogen) with a mix of random hexamers and oligodT. The cDNA was quantified using a SYBR Green qPCR kit (Roche LightCycler 480 SYBR Green I Master) and gene-specific primers. PCR was performed in 384-well plates heated at 95 °C for 10 min, followed by 45 cycles of denaturation at 95 °C for 10 s and annealing at 60 °C for 40 s. A melting curve was performed at the end of the amplification. Transcript levels were normalized to that of Actin2. All primer sequences are listed in Dataset S2.

Bisulfite Conversion and Sequencing. Total genomic DNA was extracted using DNeasy Plant Mini kit (Qiagen) following manufacturer's instructions. A total of 500–700 ng of DNA was fragmented by sonication and precipitated (with sodium acetate and ethanol). After two washes with 75% ethanol, the pellet was resuspended into 20 μL of water and further subjected to bisulfite treatment using the EpiTect Bisulfite kit (Qiagen). PCRs were performed using Taq Platinum (Invitrogen) or Taq DNA polymerase (Qiagen). PCR products were purified from gel extraction and cloned using the TOPO-TA cloning kit (pCR II-TOPO; Invitrogen). Height to 23 clones was sequenced from naïve leaf samples, whereas 15–25 clones were sequenced from mock-treated and flg22-treated leaf samples. At least three independent biological replicates were analyzed for each candidate gene/TE. The efficiency of bisulfite conversion was tested by confirming the absence of DNA methylation at a nonmethylated region. All primer sequences are listed in Dataset S2.

Cell Death Observations. Five- to 6-wk-old leaves were stained with Trypan blue. Briefly, leaves were transferred in a Trypan blue solution [10 mL lactic acid (DL Sigma; L-1250), 10 mL glycerol, 10 mL phenol, 10 mL H_2O, 10 mg Trypan blue] and boiled for 2 min. The leaves were then distained overnight in chloral hydrate and washed several times with water. Microscopic analyses were then performed using an Olympus MV 10× macrozoom and pictures were taken with a CCD camera AxioCam Mrc Zeiss.

Western Blot Analyses. Total plant protein extracts from 5- to 6-wk-old *A. thaliana* leaves treated with either water or flg22 synthetic peptide at 1 μM concentration were obtained using the Tanaka method (2) and resolved on SDS/PAGE. After electroblotting proteins on Immobilon-P membrane (Millipore), protein blot analysis was performed using antibodies raised against AGO4 and NRPE5 peptides (gifts from T. Lagrange, Laboratoire Génome et Développement des Plantes, Perpignan, France) and ACTIN8 (monoclonal antiactin plant; Sigma).

Small RNA Library/Sequencing and Data Mining. A small RNA library was made from 5- to 6-wk-old Col-0 leaf samples and deep sequenced by Fasteris (Geneva) on the Illumina HiSEq. 2000. After removing the adaptors, small RNA sequences were mapped to the *Arabidopsis thaliana* genome (TAIR10 release) using Vmatch (www.vmatch.de). Small RNAs that fully match the *Arabidopsis* genome were kept for further analyses. Sequences that are 1 kb upstream of transcription starts from flg22-induced genes were retrieved from the MIPS *A. thaliana* Genome Database (MAtDB), based on TAIR10 release. SiRNA clusters that match the promoter regions of flg22-induced genes were identified using Vmatch and are presented in Dataset S1. Results were visualized by in house Python scripts using ReportLab package (www.reportlab.com) and presented in Figs. S1, S12, and S14.

RNA Library/Sequencing and Data Mining. RNA libraries were made from 5- to 6-wk-old Col-0 leaf samples (treated with either water or flg22 at 1 μM concentration for 6 h) and deep sequenced by Fasteris (Geneva) on the Illumina HiSEq. 2000. After removing the adaptors, the sequenced were mapped on the TAIR10 version of the *A. thaliana* genome using Bowtie (parameters: quality 50, two mismatches allowed). The reads were normalized in reads per million. Results from flg22-induced NLR transcripts are presented in Dataset S1 and Fig. 4*B*.

1. Asai T, et al. (2002) MAP kinase signalling cascade in *Arabidopsis* innate immunity. *Nature* 415(6875):977–983.

2. Hurkman WJ, Tanaka CK (1986) Solubilization of plant membrane proteins for analysis by two-dimensional gel electrophoresis. *Plant Physiol* 81(3):802–806.

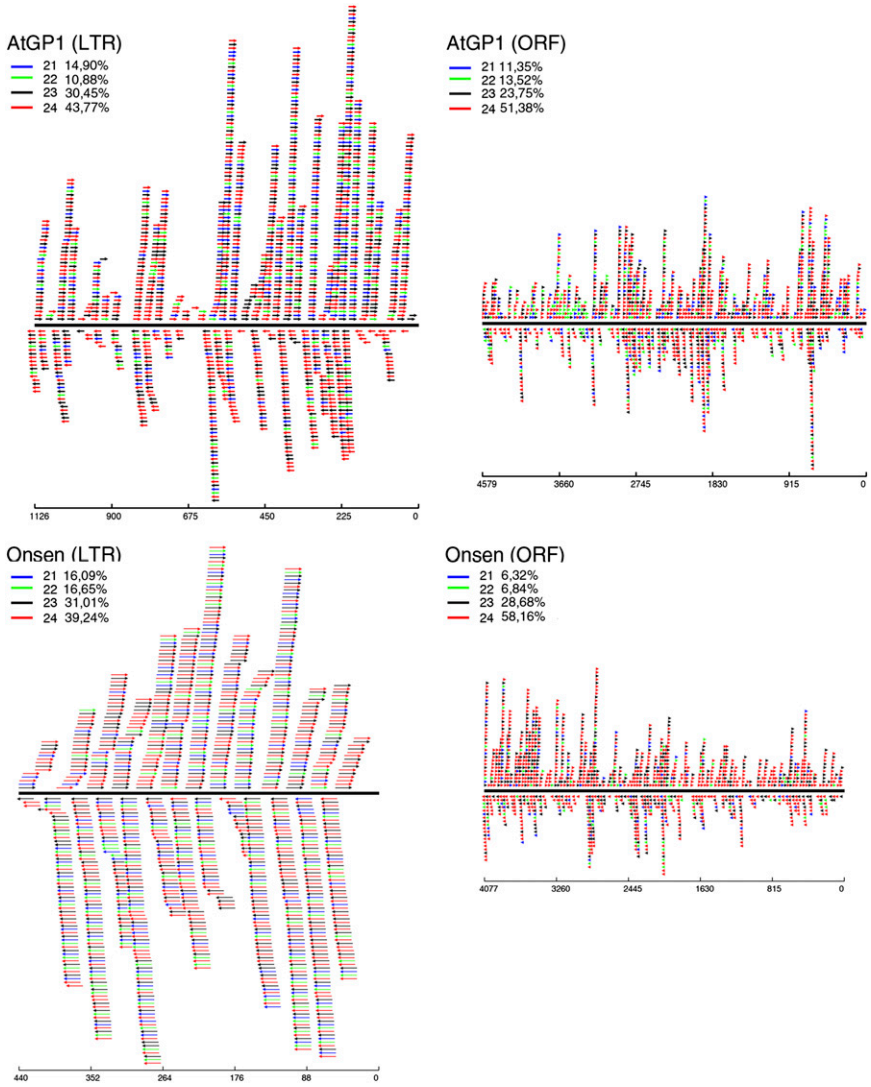

Fig. S1. *AtGP1* and *Onsen* are mostly targeted by 23- to 24-nt-long siRNAs. Schematic representation of *AtGP1* and *Onsen* long terminal repeats (LTRs) (*Left*) and *AtGP1* and *Onsen* ORFs (*Right*). A small RNA library was made from 5- to 6-wk-old WT unchallenged leaves. Small RNAs that map to the *AtGP1* (At4g03650) and the *Onsen* (At1g11265) LTR and ORF sequences are depicted.

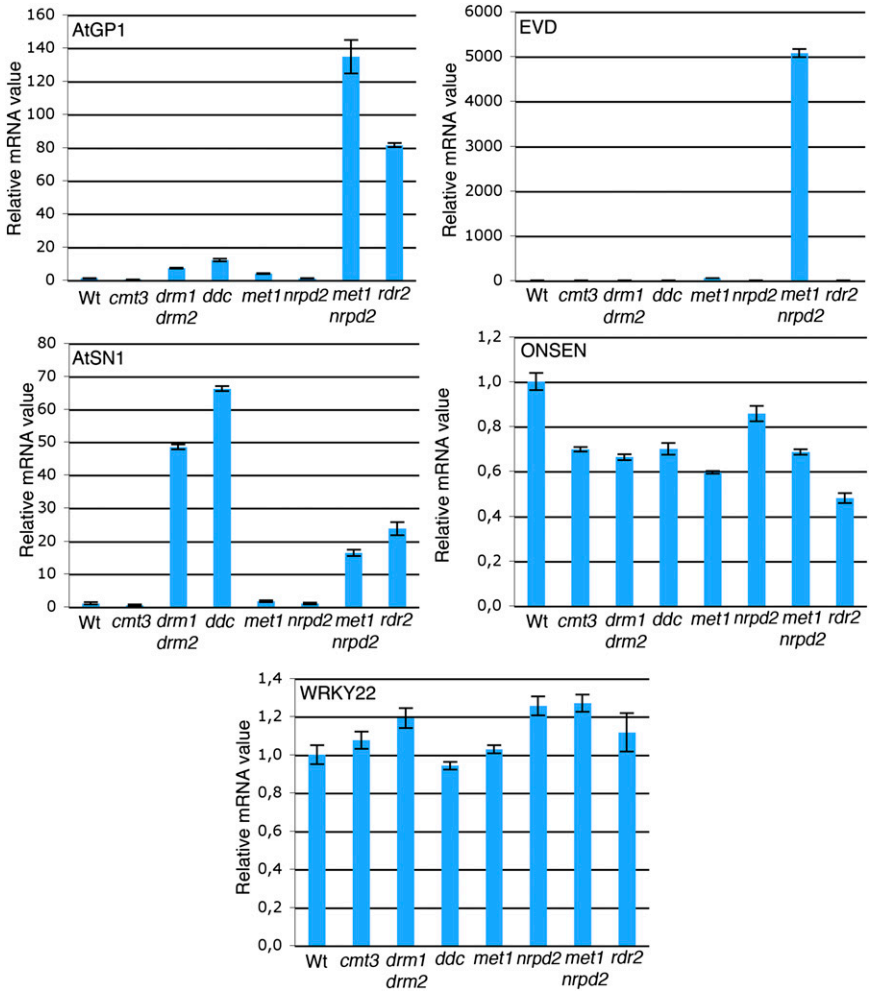

Fig. S2. Transcript accumulation of RdDM targets in DNA methylation-defective mutants. RdDM target levels were analyzed by RT-qPCR analysis. Error bars: SD from three independent PCR results. Six-wk-old leaves of WT, *cmt3-11*, *drm1-1/drm2-1*, *ddc* (*drm1-2/drm2-2/cmt3-11*), *met1-3* ($^{-/+}$), *nrpd2-2*, *met1-3* ($^{-/+}$)/*nrpd2-2*, and *rdr2-1* were used for this analysis.

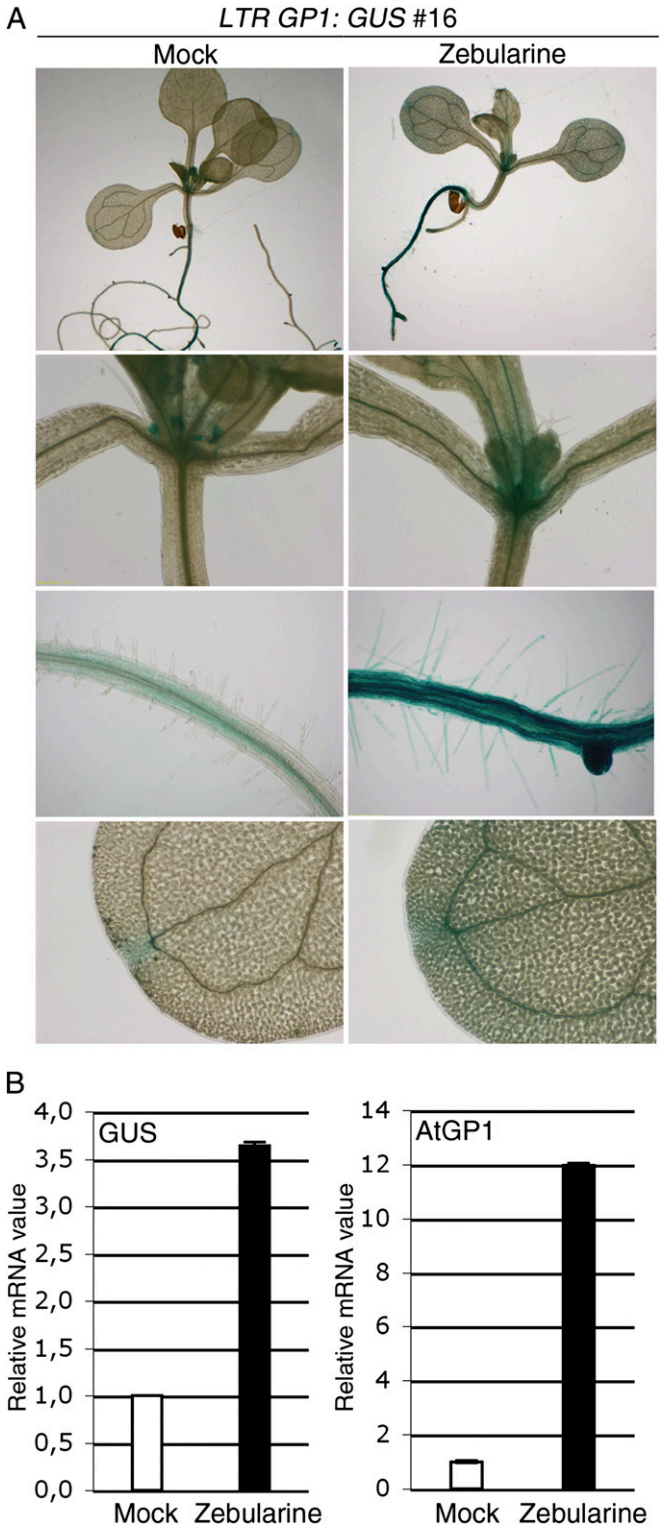

Fig. S3. The *AtGP1 LTR*:*GUS* #16 reference line is sensitive to the DNA methyltransferase inhibitor zebularine. (*A*) Pictures of histochemical GUS-stained *AtGP1 LTR*:GUS #16 seedlings grown for 14 d in the absence of zebularine (*Left*) or the presence of 40 μM of zebularine (*Right*). (*B*) RT-qPCR analyses on GUS mRNA (*Left*) and endogenous AtGP1 transcript (*Right*). Error bars: SD from three independent PCR results. Similar results were obtained in two independent experiments.

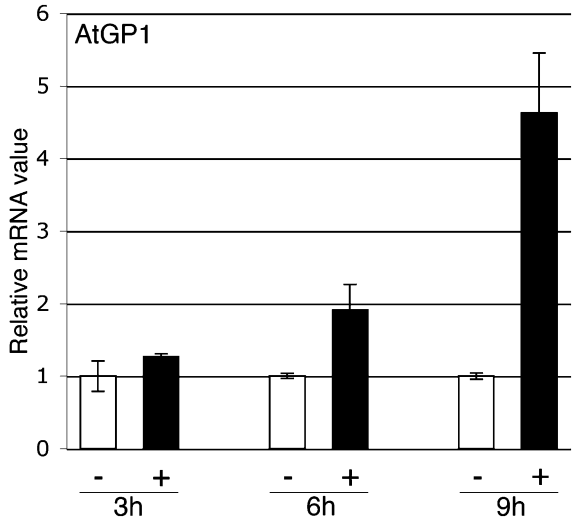

Fig. S4. Flg22 triggers an up-regulation of AtGP1 transcripts. Five- to 6-wk-old leaves of WT plants were treated with either water (–) or flg22 (+) over a 9-h time course. AtGP1 mRNA levels were monitored by RT-qPCR. Error bars: SD from three independent PCR results. Similar results were obtained in three independent experiments.

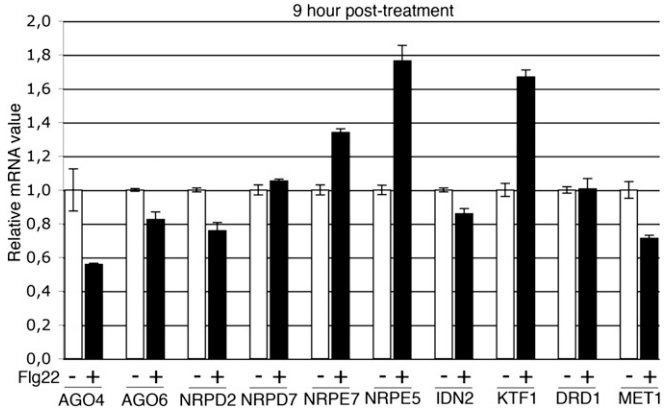

Fig. S5. The majority of flg22-sensitive TGS factor mRNAs regain normal levels at 9 h after flg22 treatment. Five- to 6-wk-old WT leaves were treated with either water (–) or flg22 (+) for 9 h and NRPD2 (Nuclear RNA polymerase D2), NRPD7 (Nuclear RNA polymerase D7), AGO4 (Argonaute 4), AGO6 (Argonaute 6), NRPE7 (Nuclear RNA polymerase E7), NRPE5 (Nuclear RNA polymerase E5), IDN2 (Involved in de novo 2), KTF1 (KOW Domain-containing transcription factor 1), DRD1 (Defective in RNA-directed DNA methylation 1), and MET1 (Methyltransferase 1) transcript levels were monitored by RT-qPCR. Error bars: SD from three independent PCR results. Similar results were obtained in three independent experiments.

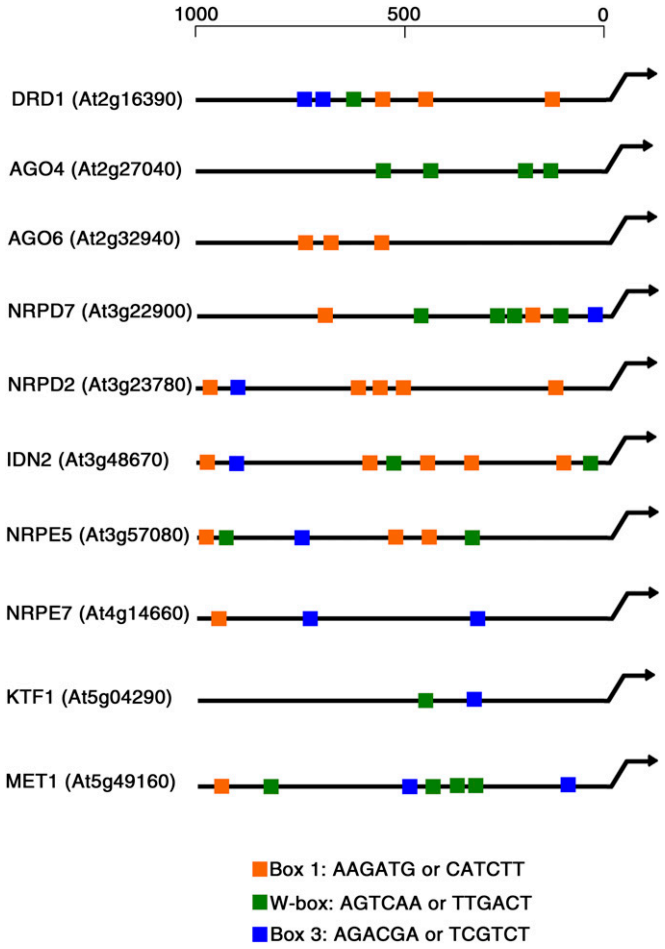

Fig. S6. Flg22-sensitive TGS factors revealed an overrepresentation of three motifs in their promoter regions. Sequences of coregulation TGS factors (1 kb upstream of the their transcription starts) were subjected to the regulatory sequence analysis tool (RSAT) computer program to retrieve putative over-represented *cis*-elements. Occurrence probabilities: Box 1 (3e-05); box 2/W-box (1,9e-04); box 3 (3,4e-04).

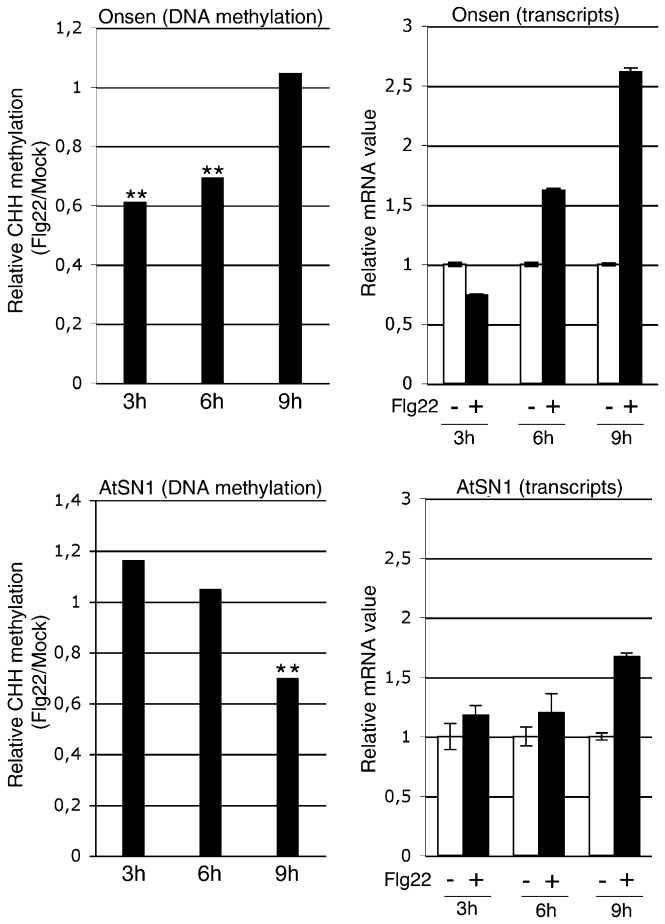

Fig. S7. Dynamics of CHH demethylation and transcript levels of Onsen and AtSN1 during flg22 elicitation. Five- to 6-wk-old WT leaves were treated with either water (–) or flg22 (+) over a 9-h time course and DNA methylation at *Onsen's* LTRs and *AtSN1* was monitored by bisulfite sequencing (*Left*). Regions analyzed at *Onsen LTR* and *AtSN1* are composed of 79 CHH and 33 CHH, respectively. Asterisks represent significant differences (**$P < 0.01$). Onsen and AtSN1 transcript levels were monitored by RT-qPCR analysis on the same samples (*Right*). Error bars: SD from three independent PCR results. Similar profiles of DNA demethylation and transcript levels were obtained in four biological replicates.

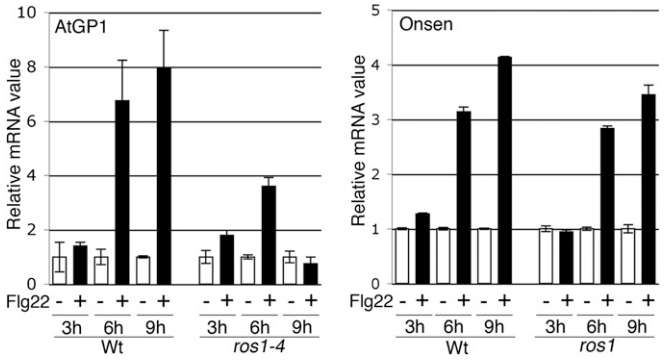

Fig. S8. *ROS1* contributes to the transcriptional reactivation of *AtGP1* but not *Onsen*. Five- to 6-wk-old WT or *ros1–4* mutant leaves were syringe infiltrated with either water (–) or flg22 (+) and mRNA levels of AtGP1 and Onsen monitored by RT-qPCR. Error bars: SD from three independent PCR results. Similar results were obtained in three independent experiments.

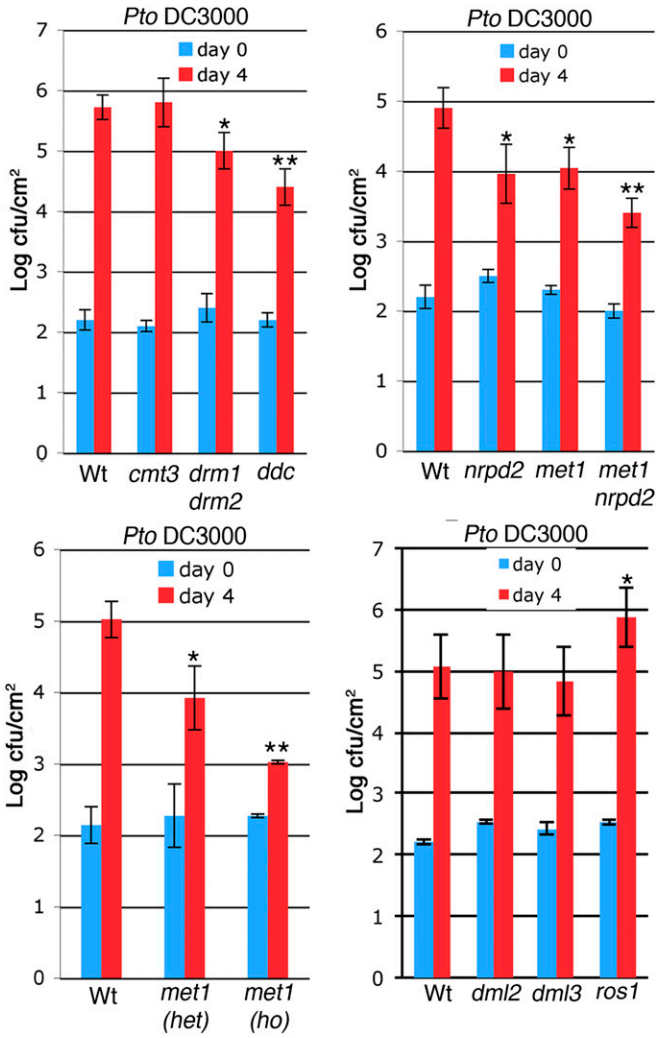

Fig. S9. DNA methylation negatively regulates resistance toward virulent *Pto* DC3000. Five- to 6-wk-old WT, *cmt3-11*, *drm1-1/drm2-1*, *ddc* (*drm1-2/drm2-2/cmt3-11*), *nrpd2-2*, *met1-3* (–/+), *met1-3* (–/+)/*nrpd2-2*, *met1-3* (–/+), *demeter-like 2* (*dml2-1*), *demeter-like 3* (*dml3-1*), *ros1-4*, and *met1-3* (–/–) leaves were syringe infiltrated with *Pto* DC3000 at 10^5 colony-forming units per milliliter (cfu/mL). Error bars: SE of log-transformed data from five independent samples. $*P < 0.05$; $**P < 0.01$, between mutants and WT. Similar results were obtained in three independent experiments.

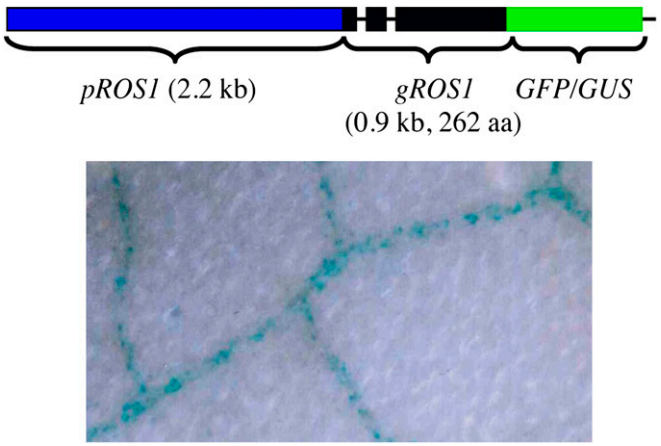

Fig. S10. *ROS1* is intensely expressed in *Arabidopsis* leaf vasculature. Schematic representation of the *ROS1p:ROS1-GUS* construct (*Upper*). Representative picture of a GUS-stained 5- to 6-wk-old leaf of the ROSp:ROS1-GUS line (*Lower*).

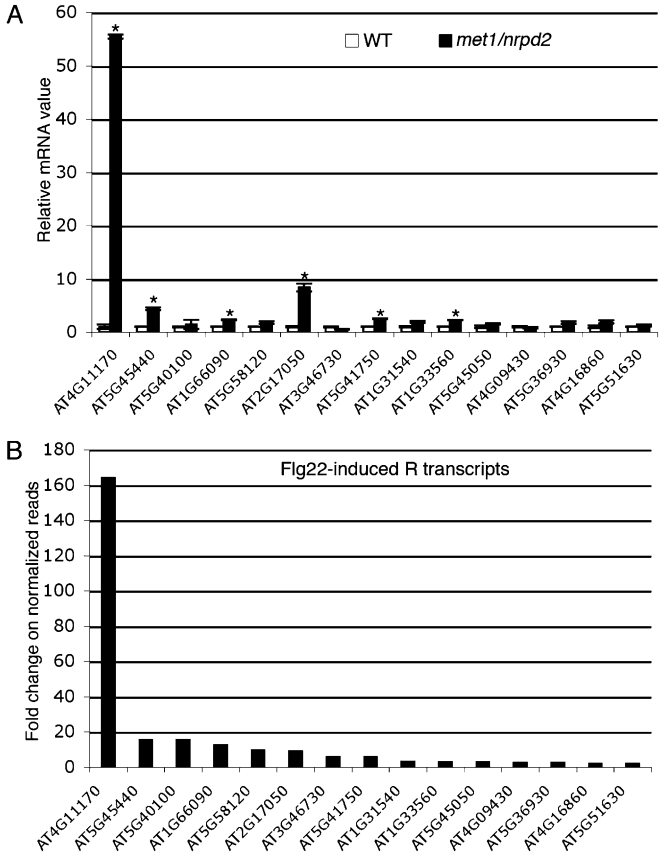

Fig. S11. *RMG1* is highly expressed in both unchallenged *met1/nrpd2* double mutant and in WT-elicited plants. (*A*) RT-qPCR in untreated WT and *met1-3*$^{(+/-)}$*/nrpd2-2* leaves of flg22-induced R gene transcripts. Asterisks represent significant differences (*$P < 0.05$). Similar results were obtained in two independent experiments. (*B*) Fold change on normalized reads from RNAseq data of flg22-induced R gene transcripts from 5- to 6-wk-old WT leaves syringe infiltrated with water (–) or flg22 (+) after 6 h.

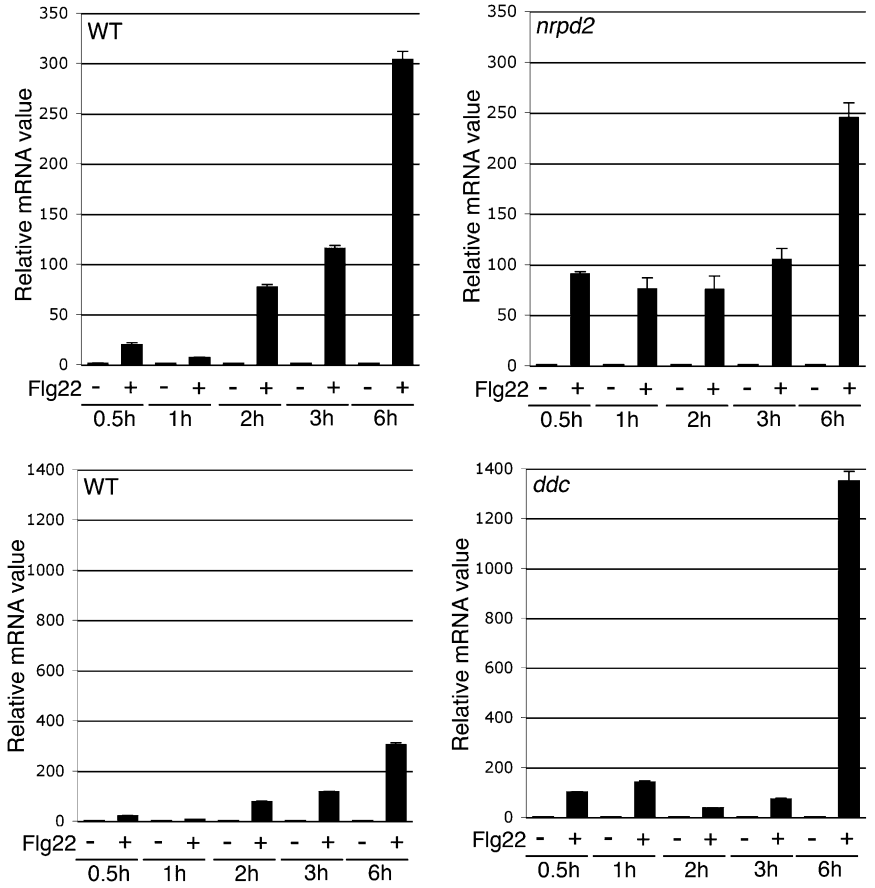

Fig. S12. RMG1 transcripts are induced earlier in mutants impaired in RdDM activity. Two-wk-old seedlings from WT, *nrpd2-2*, and *ddc* mutants were treated with either water (–) or flg22 (+; 200 nM) over a 3-h time course. RMG1 transcript levels were monitored by RT-qPCR. Error bars: SD from three independent PCR results.

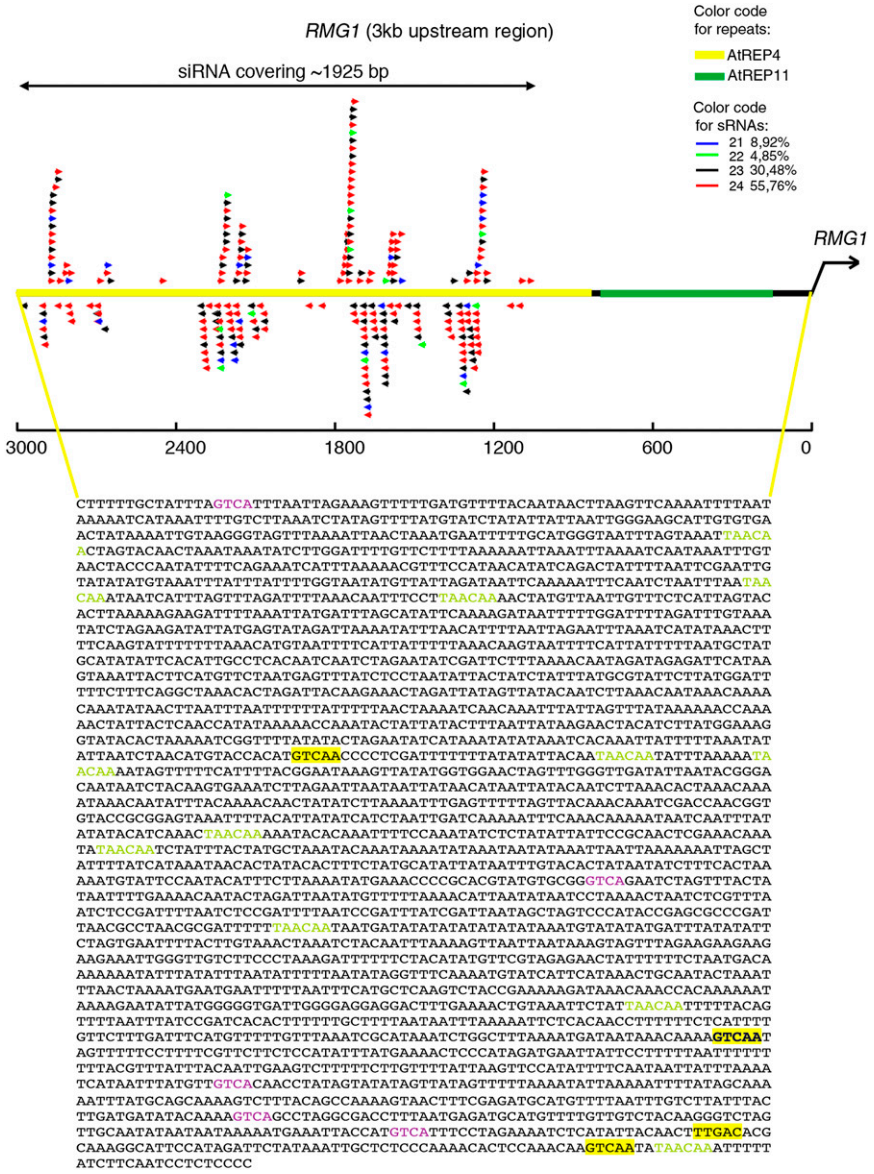

Fig. S13. Schematic representation of *RMG1* promoter. *Upper* depicts the siRNA cluster within *RMG1* promoter (3 kb upstream region from its transcription start) and the location of AtREP4 and AtREP11 repeats. Color codes are used to represent the different siRNA sizes and the two AtREP repeats. *Lower* represents the sequence of *RMG1* promoter region. Defense-responsive *cis*-elements are highlighted within this sequence; in green is the GA-responsive element (GARE), in purple is the minimum W-box motif (WRKY71OS), and in the yellow box is the stringent W-box.

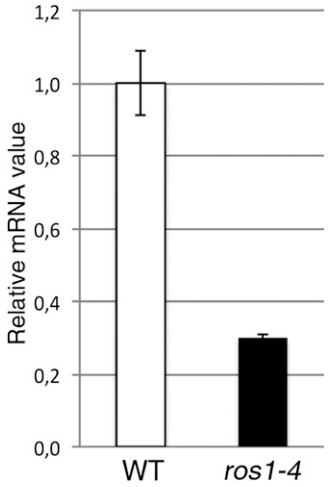

Fig. S14. RMG1 transcript levels are down-regulated in nontreated *ros1* mutant leaves. RGM1 transcript levels were monitored by RT-qPCR. Five- to 6-wk-old naïve leaves from WT and *ros1–4* mutants were used for this analysis. Similar results were obtained in three of four independent experiments.

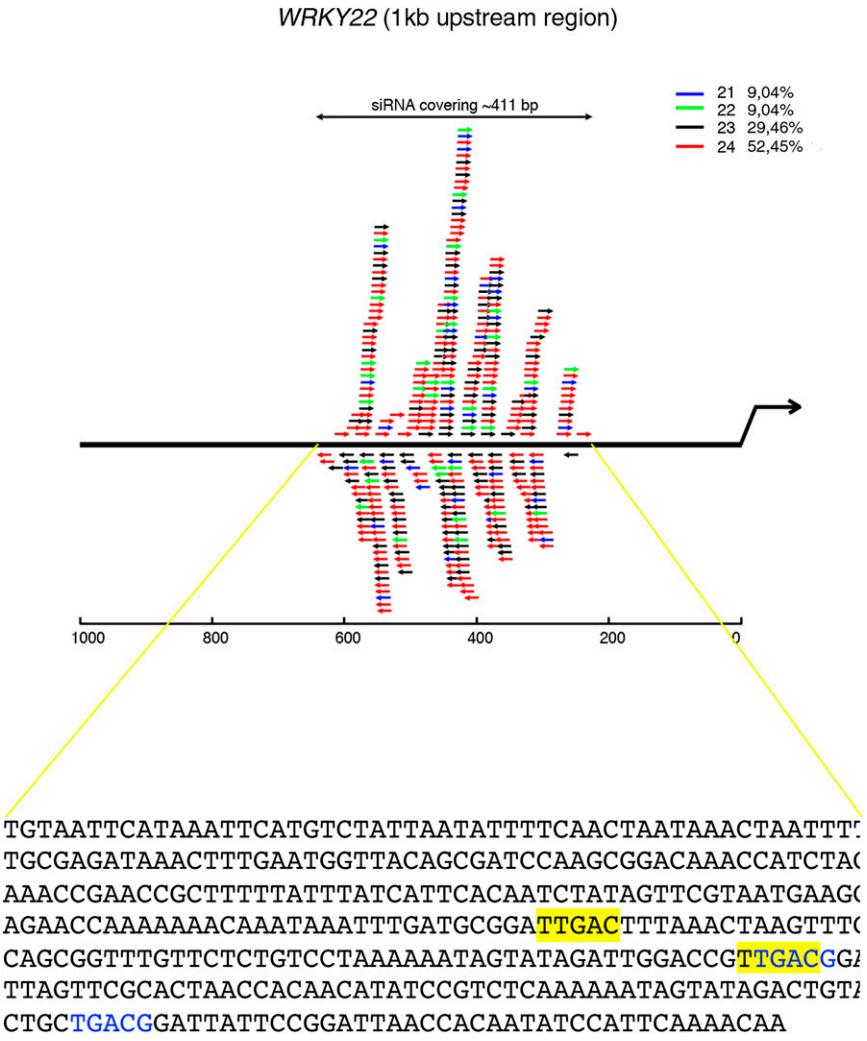

Fig. S15. Schematic representation of *WRKY22* promoter. *Upper* depicts the siRNA cluster within *WRKY22* promoter (1 kb upstream region from the transcription start). A color code is used to represent the different siRNA sizes. *Lower* represents the sequence of the undefined repeat within the *WRKY22* promoter. Defense-responsive *cis*-elements are highlighted within this sequence; in yellow is the stringent W-box and in blue is the TGA box.

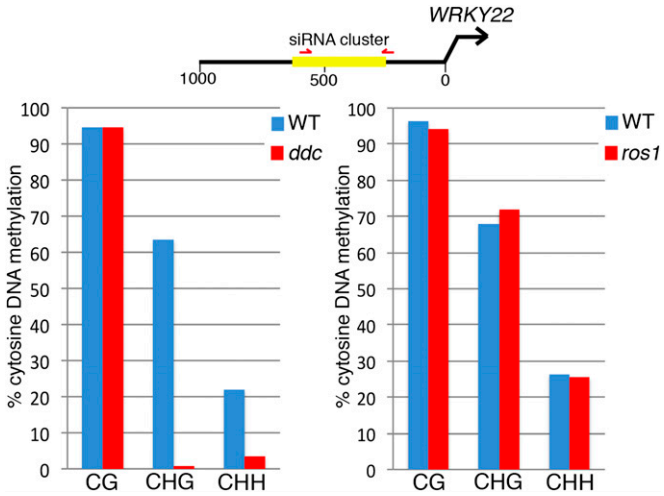

Fig. S16. DNA methylation at *WRKY22* promoter region is dependent on DNA methyltransferase- but not on *ROS1* activities. DNA methylation at the *WRKY22* promoter. Schematic representation of the *WRKY22* promoter (*Upper*) is presented where red arrows represent the position of primers used for bisulfite sequencing on WT and *ddc* leaves (*Left* graph) or WT and *ros1–4* leaves (*Right*). The region analyzed contains 14 CG, 13 CHG, and 49 CHH. Similar results were obtained in two independent experiments.

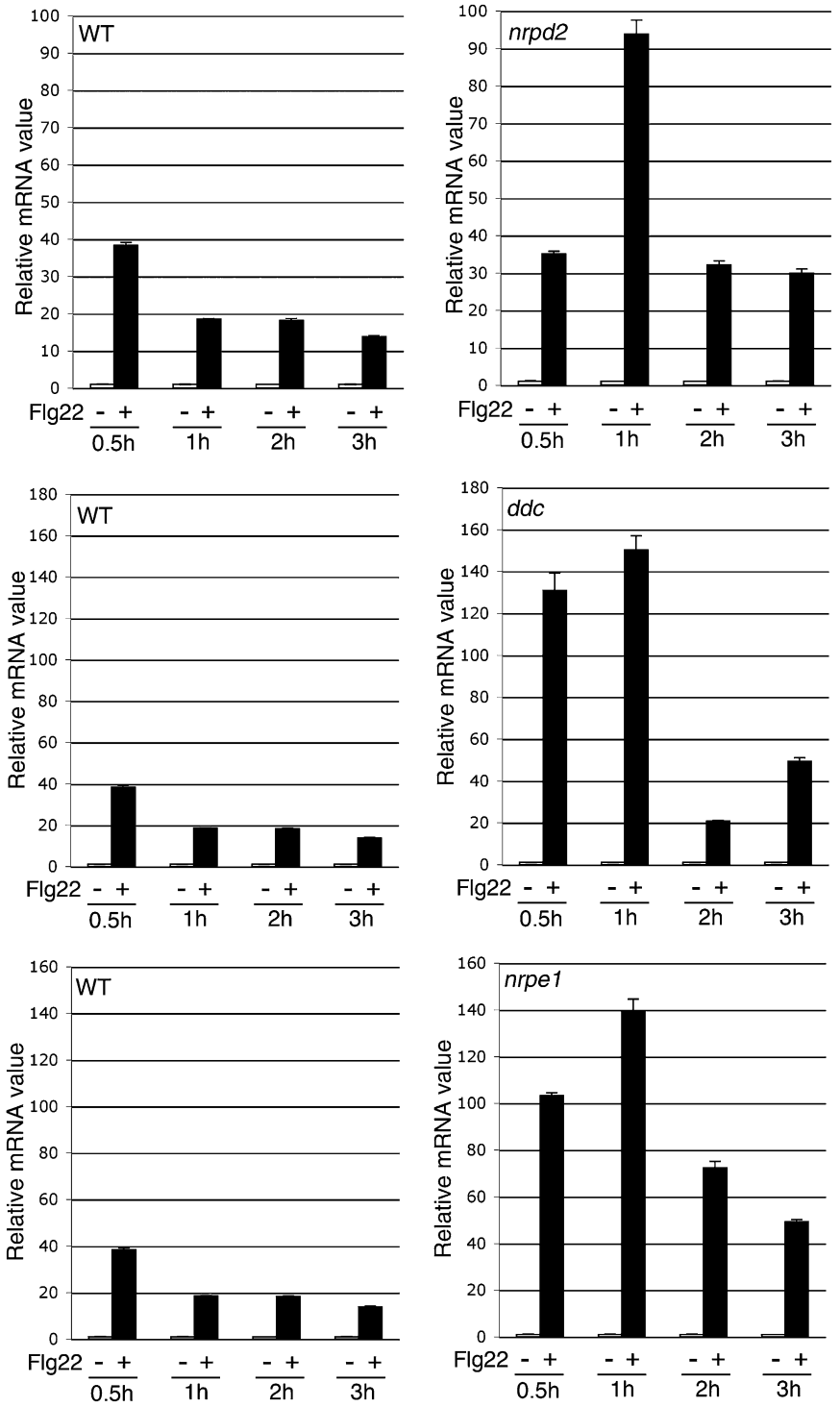

Fig. S17. WRKY22 transcripts are hyperinduced in mutants impaired in RdDM activity. Two-week-old seedlings from WT, *nrpd2-2*, *ddc*, and *nrpe1-11* were treated with either water (–) or flg22 (+; 200 nM) over a 3-h time course. WRKY22 transcript levels were monitored by RT-qPCR. Error bars: SD from three independent PCR results.

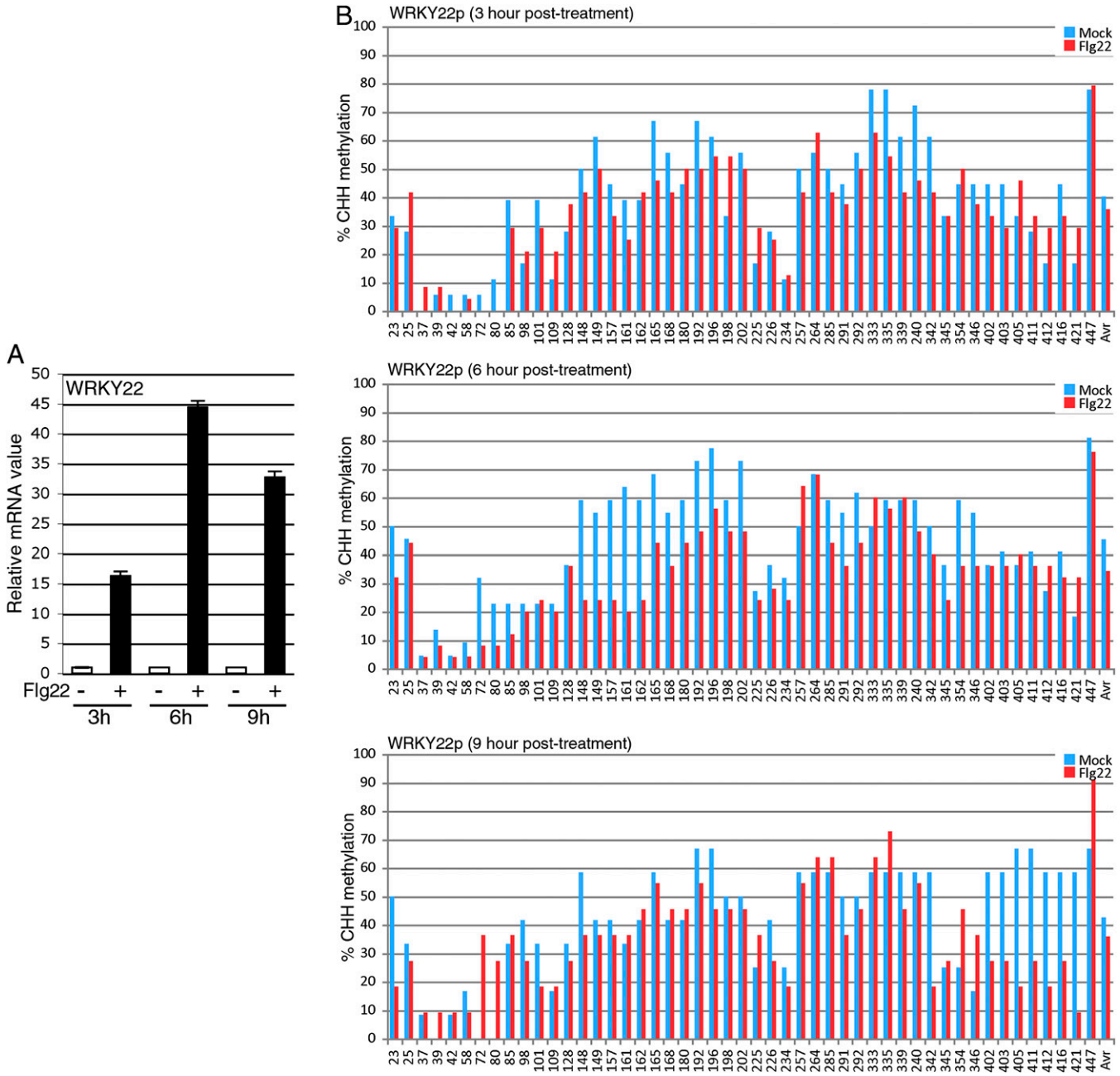

Fig. S18. Dynamics of WRKY22 transcript levels and DNA demethylation at the *WRKY22* promoter during flg22 elicitation. (*A*) Five- to 6-wk-old leaves from WT were treated with either water (–) or flg22 (+) over a 9-h time course. WRKY22 transcript levels were monitored by RT-qPCR. Error bars: SD from three independent PCR results. (*B*) DNA methylation levels at the *WRKY22* promoter monitored by bisulfite sequencing. Similar results were obtained in three independent experiments. Avr, average methylation level.

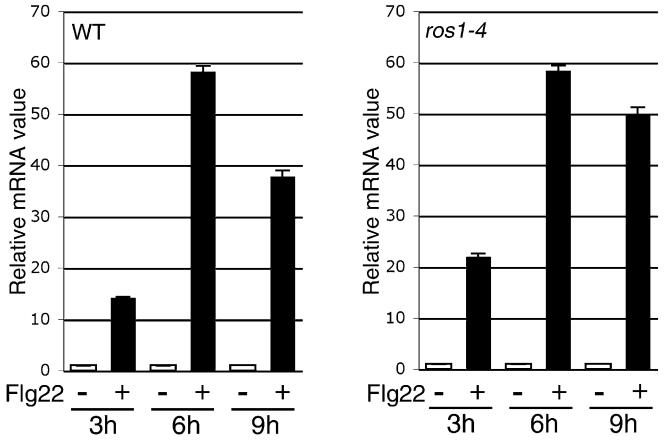

Fig. S19. Induction of *WRKY22* is unaltered in *ros1*-elicited mutant. Five to 6-wk-old leaves from WT and *ros1–4* mutants were treated with either water (–) or flg22 (+) over a 9-h time course and WRKY22 transcript levels were monitored by RT-qPCR. Error bars: SD from three independent PCR results. Similar results were obtained in three independent experiments.

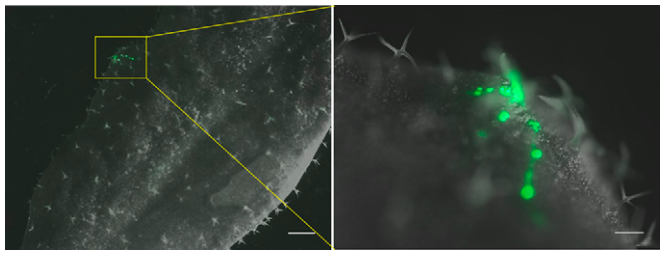

Fig. S20. *Pto* DC3000 can enter within *Arabidopsis* leaf vasculature through hydathodes. Five- to 6-wk-old leaves from WT were spray inoculated with *Pto* DC3000–GFP at a concentration of 5×10^7 cfu/mL and GFP signal was further monitored under UV light. [Scale bars, 1.5 mm (*Left*) and 0.25 mm (*Right*).] Of note, GFP signals were no longer observed 2 d after the picture was taken, indicating a strong and yet-uncharacterized antibacterial defense at the level of the hydathodes.

Other Supporting Information Files

Dataset S1 (XLS)
Dataset S2 (XLSX)
Dataset S3 (XLS)